BIOGEOCHEMICAL MODELING OF SEDIMENTS FROM THE SANTA BARBARA BASIN (CALIFORNIA)

S. Madani, F. J. R. Meysman & J. J. Middelburg

The MEDIA (Modelling Early DIAgenesis) environment is a flexible and extensible software system that provides problem-solving assistance for simulating 1D reactive transport in surface sediments. MEDIA allows multiple diagenetic models to be built by extending a template with new model components from a toolbox of available objects (elements, species, parameters, reactions). As a test, a diagenetic model was constructed to analyze an extensive sediment dataset from the Santa Barbara Basin off California. Porewater and solid phase concentration profiles were generated and compared to the available data. Concentration depth profiles were reproduced with great accuracy. The different pathways of organic matter mineralization were modeled, and the coupling among the biogeochemical cycles of C, O, N, S, Mn and Fe was investigated. This paper focuses on the coupled cycles of sulfur and iron. It illustrates the prominent role of sulfur in organic matter degradation in an anoxic environment.

Introduction

The Santa Barbara Basin (SBB) is a semi-enclosed basin of 340 to 800 m depth in the California Borderland. REIMERS *et al.* (1996) published an extensive porewater and solid phase geochemistry data set of the deep basin sites from box and kasten cores. Here we construct a diagenetic model in the MEDIA environment adequately identifying and quantifying the dominant biogeochemical processes in the SBB.

Diagenetic modelling environment

The MEDIA software environment was developed to simulate the coupling of geochemical, physical and biological processes in surface sediments. The MEDIA software allows user-tailored models to be built from a set of basic building blocks and provides an efficient numerical solution for these models. A detailed review of the transport and reaction components is given in MEYSMAN *et al.* (in press).
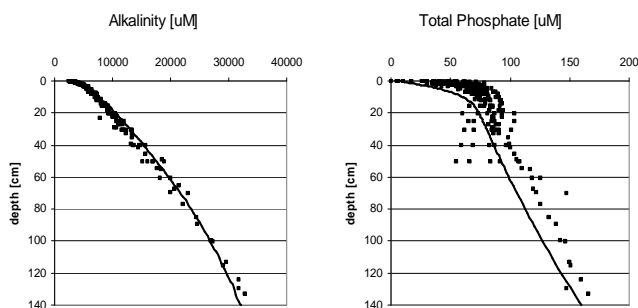

Fig. 1. In the first few centimeters, the alkalinity (a proxy for total carbonate), total ammonium (not shown) and total phosphate profiles show a strong curvature, indicating a strong remineralization of organic matter. In order to reproduce this curvature, we had to assume a considerable labile fraction of organic matter with a decay constant of 2.0 yr^{-1}. In addition, two refractive types were included with decay constants of 0.06 yr^{-1} and 1.10^{-4} yr^{-1}, respectively (see Fig. 2a for OM depth profile combining all three fractions). As can be seen from the alkalinity, total ammonium and total phosphate profiles, there is a strong influx at their lower boundary, indicating a zone of intense geochemical activity just below the modeled stratum.

Concentration depth profiles

Fig. 1 compares the steady-state resulting output of the model with the data profiles. The steady-state model profiles of both porewater constituents and solid-phase constituents closely fit the observations, indicating that the model explains a substantial part of the geochemical complexity in the SBB.

Organic matter is modeled as three fractions, with different first-order degradation rates and distinct C/N/P ratios, to account for the decreasing reactivity and preferential re-mineralization of C-N-rich compounds with depth. The kinetic reactions include the mineralization of organic matter, the re-oxidation of reduced byproducts formed in the mineralization, the reduction of manganese and iron (hydr)oxides by sulfides, the formation of iron sulfide and pyrite, the precipitation of manganese and calcium carbonate. The equilibrium reaction set includes the common acid-base equilibria in the porewater and adsorption of ammonium, phosphate, soluble iron and manganese onto the sediment matrix. The values of the equilibrium constants and the kinetic constants used in the simulation are found in MEYSMAN *et al.* (in press).

OM mineralization pathways

The model estimates the total mineralization rate (i. e. the combined rate of all three fractions integrated over depth) at 145 $\mu mol\ C\ cm^{-2}yr^{-1}$. The rates attributed to the different mineralization pathways are shown in Table 1. Sulfate reduction is by far the dominant pathway, and Fig. 2b compares the Sulfate Reduction Rate (SRR) obtained from ^{35}S incubations, with the modeled SRR. A good fit to the observations is obtained, except for the first two centimeters. This is the zone where the labile organic matter is processed, resulting in a sharp peak in the SRR. Possibly due to insufficient resolution, this peak is not observed in the SRR data.

Carbon degradation	Reaction rate ($\mu mol\ C\ cm^{-2}\ yr^{-1}$)	%	Reference
$\{CH_2O\} + O_2 \rightarrow CO_2 + H_2O$	20.72	14.29	[1]
$\{CH_2O\} + 0.8\ NO_3^- + 0.8\ H^+ \rightarrow CO_2 + 0.4\ NO_2 + 1.4\ H_2O$	28.13	19.39	[2]
$\{CH_2O\} + 2\ MnO_2 + 4\ H^+ \rightarrow 2\ Mn + CO_2 + 3\ H_2O$	0.99	0.69	[3]
$\{CH_2O\} + 4\ FeOOH + 8\ H^+ \rightarrow 4\ Fe + CO_2 + 7\ H_2O$	9.41	6.49	[4]
$\mathbf{\{CH_2O\} + 0.5\ SO_4^{2-} + 0.5\ H^+ \rightarrow 0.5\ HS^- + CO_2 + H_2O}$	**82.39**	**56.81**	**[5]**
$\{CH_2O\} \rightarrow 0.5\ CO_2 + 0.5\ CH_4$	3.39	2.34	[6]

Table 1. In the surface sediments organic carbon can be degraded in six different ways. Denitrification [2] and sulfate reduction [5] constitute the dominant pathways (20% and 56%, respectively). Despite the low bottom-water concentrations, oxic mineralization [1] still accounts for 14% of the organic matter degradation. Methanogenesis [6] and iron reduction [4] only comprise minor pathways, whereas the manganese oxide pathway [3] can virtually be neglected.
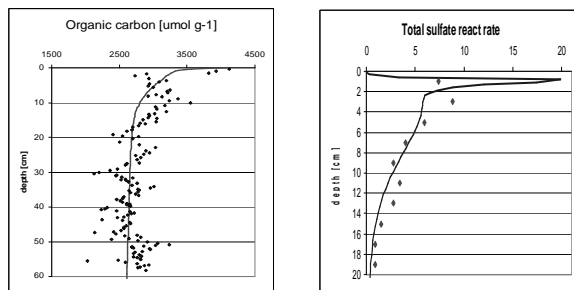

Fig. 2. OM profiles (a) and ^{35}S incubation and modeled SRR (b).

Sulfur and iron cycling

Fig. 3 shows that the main source of sulfur in the sediment comes from the water column through influx of SO_4^{2-}. A third of this incoming SO_4^{2-} flux is transferred to deeper lying sediment below 140 cm. As can be seen from the SO_4^{2-} porewater profile (Fig. 1), strong sulfate consumption takes place just below our modeled sediment stratum, presumably due to the oxidation of a significant flux of methane diffusing

upwards [1]. The remaining two thirds of the incoming SO_4^{2-} flux is used for sulfate reduction, mostly through direct mineralization of C_{org}. Nevertheless, some sulfate is used to oxidize H_2 [2], a highly reactive intermediate in the OM mineralization process, although resulting here from pyrite formation. Sulfate reduction produces HS^-, of which equal amounts are engaged in FeS formation on the one hand [3] and the acid-base equilibrium with H_2S on the other [4]. The latter combines with FeS to produce pyrite [5]. Within the modeled stratum, all the FeS formed is converted into pyrite, resulting in a significant burial of sulfur. Looking at the sulfide fluxes to and from the sediment, some is coming from deeper layers (presumably produced by methane oxidation through sulfate), whereas three times that amount is transferred across the sediment-water interface. The latter flux of sulfide into the water column then produces the suboxic to anoxic conditions observed in the lower water column of the SBB.

Black arrows represent geochemical reactions that take place in surface sediments. Green arrows show the fluxes across the water-sediment interface and the surface sediment-deep sediment interface. The unit of the figures is $\mu mol\ C\ cm^{-2}\ yr^{-1}$.

Due to the importance of sulfate reduction, we took a closer look at the cycling of sulfur within the modeled stratum. Because iron is a key player in the sulfur cycle due to precipitation of FeS and FeS_2, we also looked at the Fe cycle. Table 2 lists the most important reactions involved in these two cycles.
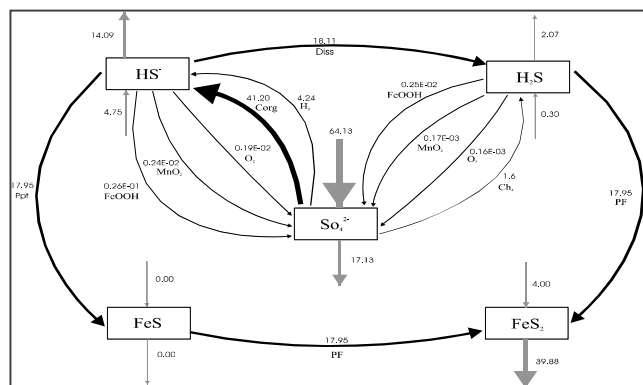

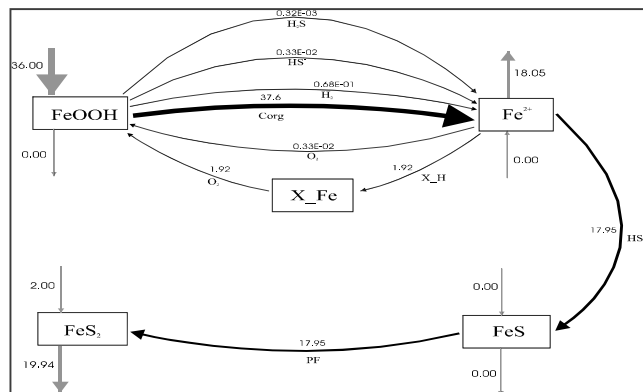
Fig. 3. Main sources of sulfur in the sediment

Fig.4. The iron cycle in the sediment.

Fig. 4 shows that the main supply of iron in the sediment comes from the water column through the deposition of solid FeOOH. There is also a recycling of FeOOH through the oxidation of particles containing iron (X_Fe) [6]. This iron oxide is reduced mainly *via* the mineralization of C_{org}, and only a negligible fraction combines with hydrogen and hydrogen sulfide. The ferrous iron (Fe^{2+}) produced is engaged partly in FeS formation and the subsequent burial of pyrite on the one hand [3]. On the other hand, Fe^{2+} partly diffuses to the overlying water column, where it contributes to the anoxia of the overlying water through scavenging of molecular oxygen. Consequently, there is only a minor recycling pathway of Fe^{2+}

to FeOOH within the sediment (*via the adsorption of Fe^{2+} to the matrix and the subsequent oxidation of this X_Fe+*). Most of the Fe^{2+} recycling is displaced to the overlying water.
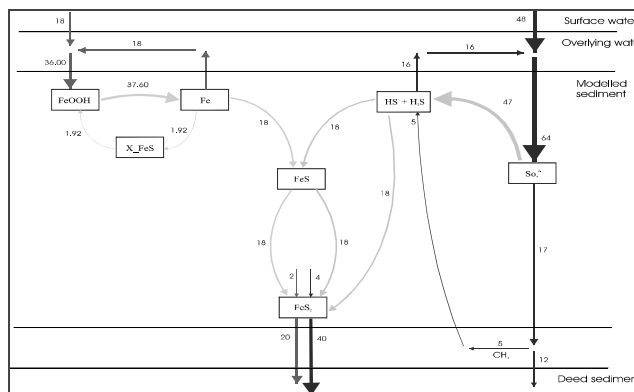

Fig. 5. Simplified scheme of coupled sulfur and iron cycles.

Coupling between S and Fe

Fig. 5 shows the coupling of the Fe and S cycles. In addition to the transformations within the modeled sediment stratum, we also tentatively depicted the cycling within the overlying bottom water as well as the presumed transformations in the reactive zone just below the modeled sediment layer. In the case of iron, 10% enters the BBL as pyrite (FeS_2), whereas the other 90% arrives as iron (hydr)oxides (FeOOH). In the end, all iron is buried as pyrite. In the case of sulfur, all enters the BBL as sulfate, and roughly 80% is buried as pyrite. Surprisingly, about 20% of the sulfur is buried in reduced form other than pyrite (elemental and organic S).

Reactions	Reference
$SO_4^{2-} + CH_4 \rightarrow CO_2 + H_2S$	[7]
$SO_4^{2-} + 4,5\ H_2 \rightarrow HS^- + 4\ H_2O$	[8]
$HS^- + Fe^{2+} \rightarrow FeS + H^+$	[9]
$HS^- + H^+ \rightarrow H_2S$	[10]
$FeS + H_2S \rightarrow FeS_2 + H_2$	[11]
$X\_H + Fe \rightarrow X\_Fe + H$	[12]

Table 2. Summary of the reactions described above.

References

KUWABARA, J. S., VAN GEEN, A., MCCORKLE, D. C. & BERNHARD, J. M. (1999) Geochim. Cosmochim. Acta, **63**, 2199-2209.
REIMERS, C. E., RUTTENBERG, K. C., CANFIELD, D. E., CHRISTIANSEN, M. B. & MARTIN J. B., 1996. Geochim. Cosmochim. Acta **60**, 4037-4057.
Meysman, F. J. R., Middelburg, J. J., Herman, P. M. J. & Heip, C .H. R. (in press) Reactive transport in surface sediments. II. MEDIA: an object-oriented problem-solving environment for early diagenesis. Comp. Geosci.

S. Madani, F. J. R. Meysman & J. J. Middelburg, Centre for Estuarine and Marine Ecology (CEME), The Netherlands Institute of Ecology (NIOO), Korringaweg 7, NL-4401 NT Yerseke; e-mail: s.madani@nioo.knaw.nl.